Interfacial Engineering of Metal Organic Frameworks Derived Hierarchical CoP-Ni_5P_4 Nanosheet Arrays for Overall Water Splitting

Jiahui Jiang[a], Guancheng Xu[a], Yang Li[a], Can Wang[a], Li Zhang[a,b]*

a. State Key Laboratory of Chemistry and Utilization of Carbon Based Energy Resources; College of Chemistry, Xinjiang University, Urumqi, 830017, Xinjiang, PR China.

b. College of Chemical Engineering, Xinjiang University, Urumqi, 830017, Xinjiang, PR China.

* Corresponding author

E-mail: zhangli420@xju.edu.cn

Experimental section

Chemicals and reagents

Cobalt(II) nitrate hexahydrate ($Co(NO_3)_2·6H_2O$, 98%) and sodium hypophosphite ($NaH_2PO_2·H_2O$, 99%) were provided by Tianjin Yongsheng Fine Chemical Company. Formic acid (HCOOH, 88 wt%) and methylamine water solution (CH_3NH_2, 30 wt%) were provided by Tianjin Zhiyuan Chemical Plants. Nickel foam (NF) was provided by Changsha Lyrun Material Co., Ltd. All chemical reagents were used without further purification.

Material characterization

X-ray diffraction was collected on a Bruker D8 advance diffractometer with monochromatized Cu Kα radiation (λ = 0.154 05 nm). Field-emission scanning

electron microscopy, energy-dispersive X-ray spectroscopy and elemental mapping were taken on Hitachi S-4800 microscope. Transmission electron microscopy was taken on Hitachi H600 microscope. X-ray photoelectron spectroscopy (XPS) was measured on an Escalab 250 Xi system (Thermo Fisher Scientific).

Electrochemical characterization

All electrochemical tests were performed on a CHI760E electrochemical workstation (Shanghai Chenhua Instrument Co. Ltd.). A standard three-electrode system was used with the prepared CoP-Ni_5P_4/NF electrode as the working electrode (the geometric area is 0.5 cm^2), a standard Ag/AgCl electrode (saturated KCl solution) as the reference electrode, a graphite rod as the counter electrode, and 1 M KOH solution as the electrolyte. All potentials reported were calibrated to the reversible hydrogen electrode (RHE) : $E_{RHE} = E_{Ag/AgCl} + 0.198 + 0.059 \times pH$, pH = 13.6 for 1 M KOH. OER and HER polarization curves were recorded at a scan rates of 1 and 5 mV s^{-1}, respectively. Tafel slopes were calculated based on polarization curves. As for overall water splitting, the prepared CoP-Ni_5P_4/NF electrode were directly used as cathode and anode in a two-electrode configuration in 1.0 M KOH at room temperature. The C_{dl} of the samples were measured via a simple CV method to indicate the electrochemically active surface areas (ECSA). The EIS measurements were recorded with a frequency range from 0.01 kHz to 100 Hz. The long-term electrochemical stability was performed using constant voltage measurements of 10 mA cm^{-2} for all relevant reactions: HER, OER, and overall water splitting.

Calculation of turnover frequency: The TOF values of CoP-Ni_5P_4/NF,

CoP+Ni_5P_4/NF, CoP and Ni_5P_4/NF were calculated according to equation: TOF = $j \times A/(e \times F \times m)$, where j is the current density obtained at overpotential of 240 mV, A is the surface area of the NF electrode (0.25 cm^2), F is the Faraday efficiency (96,485 C mol^{-1}) and m is the number of moles of the CoP-Ni_5P_4/NF and CoP ink drips onto Ni_5P_4/NF electrodes.

Theoretical calculation method and Model

The CoP (001), Ni_5P_4 (010) and CoP (001) - Ni_5P_4 (010) surfaces were built, where the vacuum space along the z direction is set to be 18 Å, which is enough to avoid interaction between the two neighboring images. Then OH ,O and OOH groups were loaded on the surface. The bottom three atomic layers were fixed, the top three atomic layers were relaxed adequately. The first principles calculations in the framework of density functional theory were carried out based on the Cambridge Sequential Total Energy Package known as CASTEP[1]. The exchange-correlation functional under the generalized gradient approximation (GGA)[2] with norm-conserving pseudopotentials and Perdew-Burke-Ernzerhof functional was adopted to describe the electron-electron interaction[3]. An energy cutoff of 750 eV was used and a k-point sampling set of 7 × 7 × 1 were tested to be converged. A force tolerance of 0.01 eV $Å^{-1}$, energy tolerance of 5.0×10^{-7} eV per atom and maximum displacement of 5.0×10^{-4} Å were considered. The Grimme method for DFT-D correction is considered for all calculations[4].

Adsorption energy ΔE of A (= OH, O and OOH) group on the surface of substrates was defined as[5,6]:

$$\Delta E = E_{*A} - (E_{*} + E_{A}) \quad \text{(S1)}$$

where *A and * denote the adsorption of A group on substrates and the bare substrates, E_A denotes the energy of A group.

Gibbs free energy change (ΔG) of each chemical reaction is calculated by:[5, 6]

$$\Delta G = \Delta E + \Delta ZPE - T\Delta S \quad \text{(S2)}$$

where E, ZPE, T and S denote the calculated total energy, zero point energy, temperature and entropy, respectively. Here, T = 300 K is considered.

The adsorption energies follow the approach:

$$\Delta E_{*O} = E\,(\text{sub/O}) - E\,(\text{sub}) - [E\,(H_2O) - E\,(H_2)] \quad \text{(S3)}$$

$$\Delta E_{*OH} = E\,(\text{sub/OH}) - E\,(\text{sub}) - [E\,(H_2O) - E\,(H_2)/2] \quad \text{(S4)}$$

$$\Delta E_{*OOH} = E\,(\text{sub/OOH}) - E\,(\text{sub}) - [2\times E\,(H_2O) - 3\times E\,(H_2)/2] \quad \text{(S5)}$$

where E (sub/O), E (sub/OH) and E (sub/OOH) denote the total energies of O, OH and OOH groups on substrate. E (sub), E (H_2O) and E (H_2) are the total energies of bare substrate, water, and hydrogen gas, respectively.

The electrochemical model of OER can be divided into four one–electron reactions:

$$H_2O + * \rightarrow *OH + (H^+ + e^-) \quad \text{(S6)}$$

$$*OH + (H^+ + e-) \rightarrow *O + 2(H^+ + e^-) \quad \text{(S7)}$$

$$H_2O + *O + 2(H^+ + e^-) \rightarrow *OOH + 3(H^+ + e^-) \quad \text{(S8)}$$

$$*OOH + 3(H^+ + e^-) \rightarrow O_2 + * + 4(H^+ + e^-) \quad \text{(S9)}$$

The detailed Gibbs free energy changes of steps S6-S9 can be calculated by:

$$\Delta G_1 = \Delta G_{*OH} - eU \quad \text{(S10)}$$

$$\Delta G_2 = \Delta G_{*O} - \Delta G_{*OH} - eU \quad \text{(S11)}$$

$$\Delta G_3 = \Delta G_{*\mathrm{OOH}} - \Delta G_{*\mathrm{O}} - \mathrm{e}U \quad \text{(S12)}$$

$$\Delta G_4 = 4.92\mathrm{eV} - \Delta G_{*\mathrm{OOH}} - \mathrm{e}U \quad \text{(S13)}$$

where the sum of $\Delta G_{1\text{-}4}$ is fixed to the negative of experimental Gibbs free energy of formation of two water molecules ($-2^{\Delta_{H_2O}^{exp}} = 4.92$ eV). The Gibbs free energy of ($H^+ + e^-$) in solution is estimated as the half energy of H_2 molecule at standard condition.[7]

The overpotential of OER is determined by following equations:

$$\eta_{\mathrm{OER}} = U_{\mathrm{OER}} - 1.23 \quad \text{(S14)}$$

$$U_{\mathrm{OER}} = \mathrm{Max}\,(\Delta G_{*\mathrm{OH}}, \Delta G_{*\mathrm{O}} - \Delta G_{*\mathrm{OH}}, \Delta G_{*\mathrm{OOH}} - \Delta G_{*\mathrm{O}}, 4.92\mathrm{eV} - \Delta G_{*\mathrm{OOH}}) / \mathrm{e} \quad \text{(S15)}$$

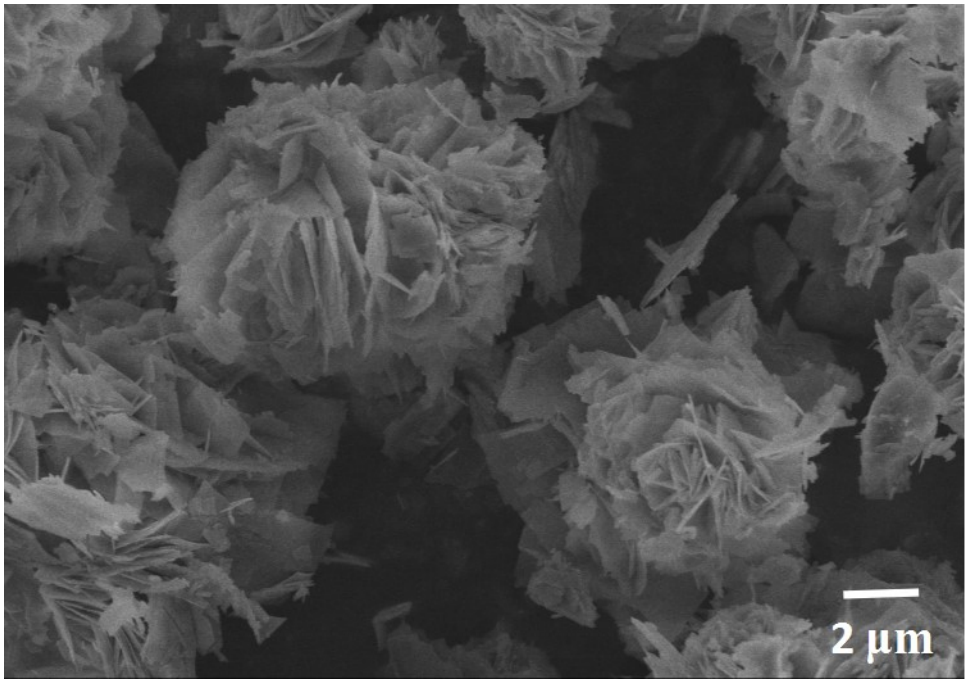

Figure S1. FESEM image of Co-FF.

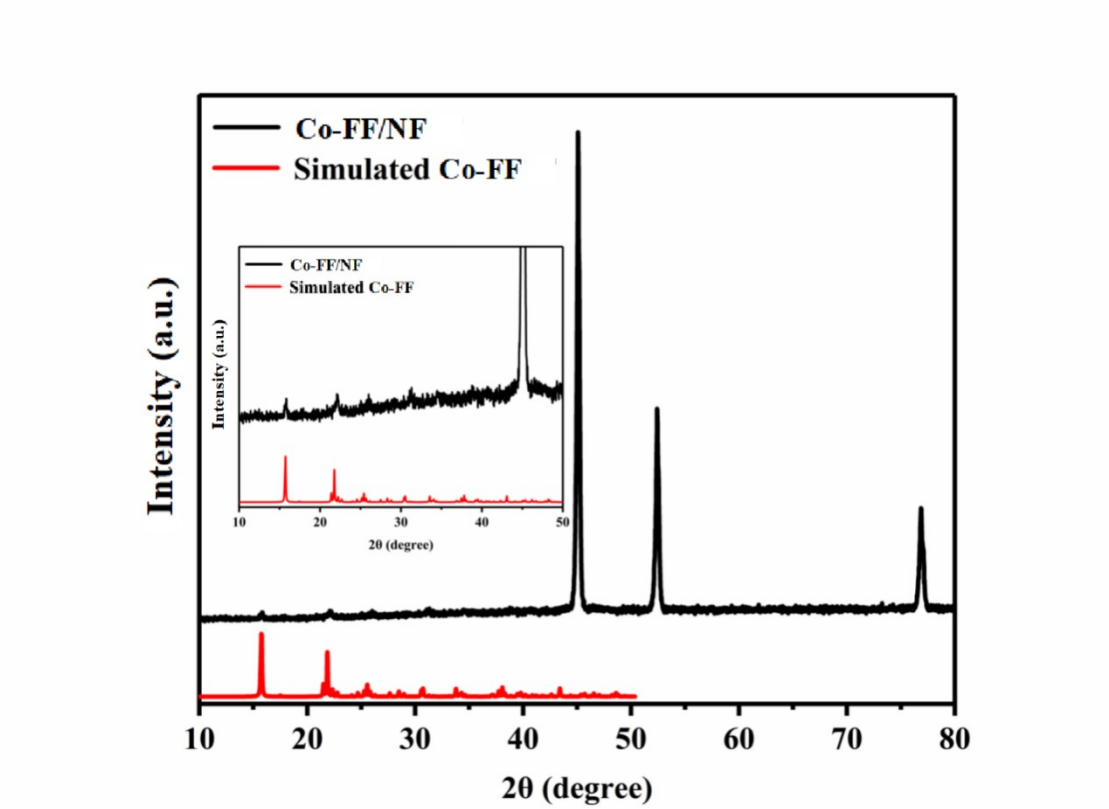

Figure S2. XRD pattern of Co-FF/NF.

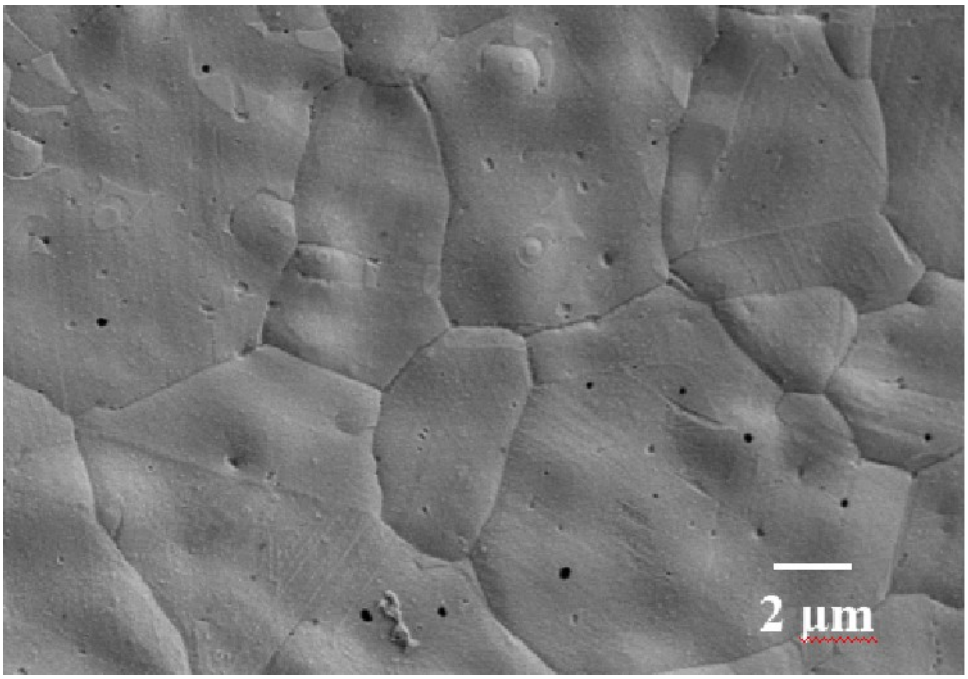

Figure S3. FESEM image of FM/NF.

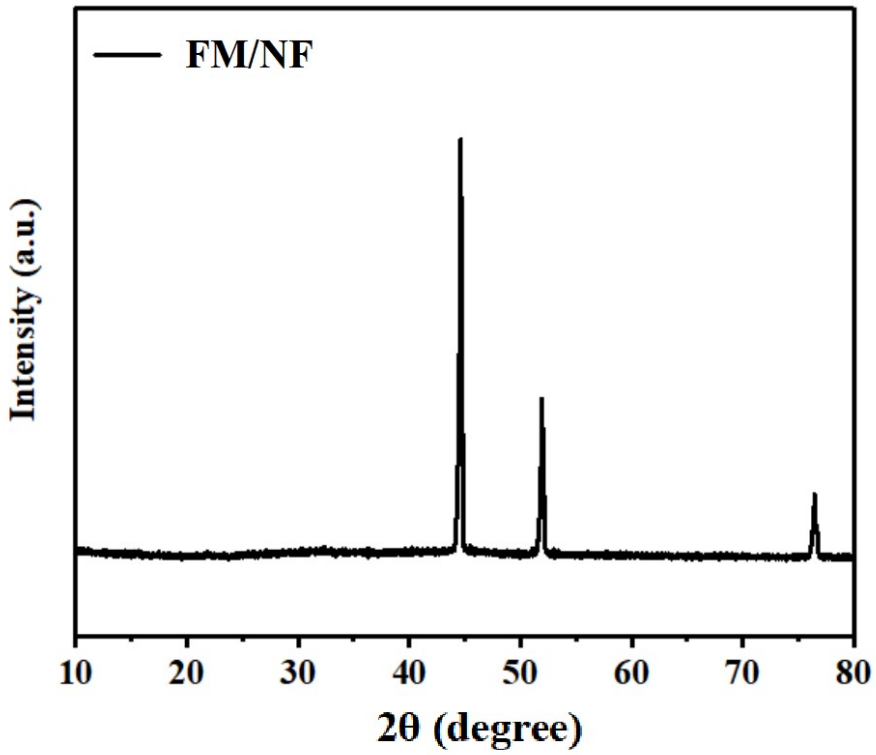

Figure S4. XRD pattern of FM/NF.

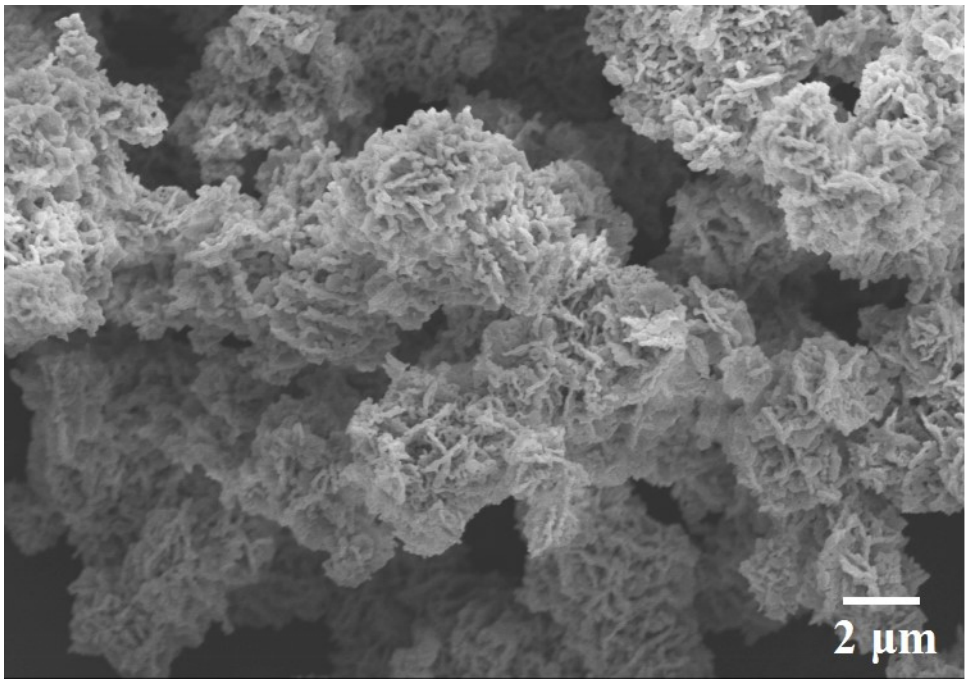

Figure S5. FESEM image of CoP.

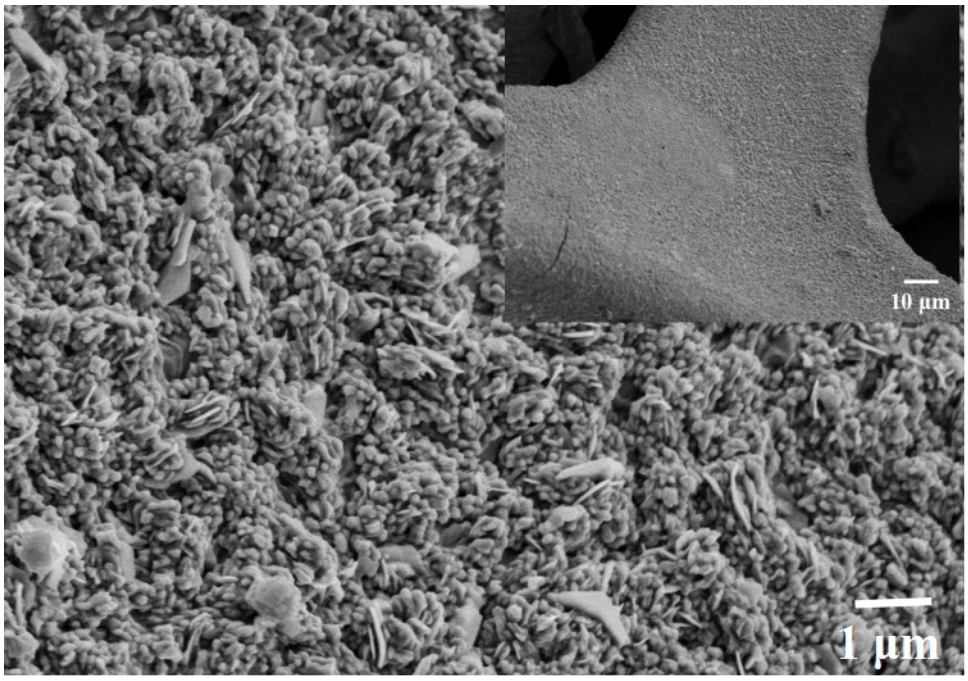

Figure S6. FESEM image of Ni_5P_4/NF.

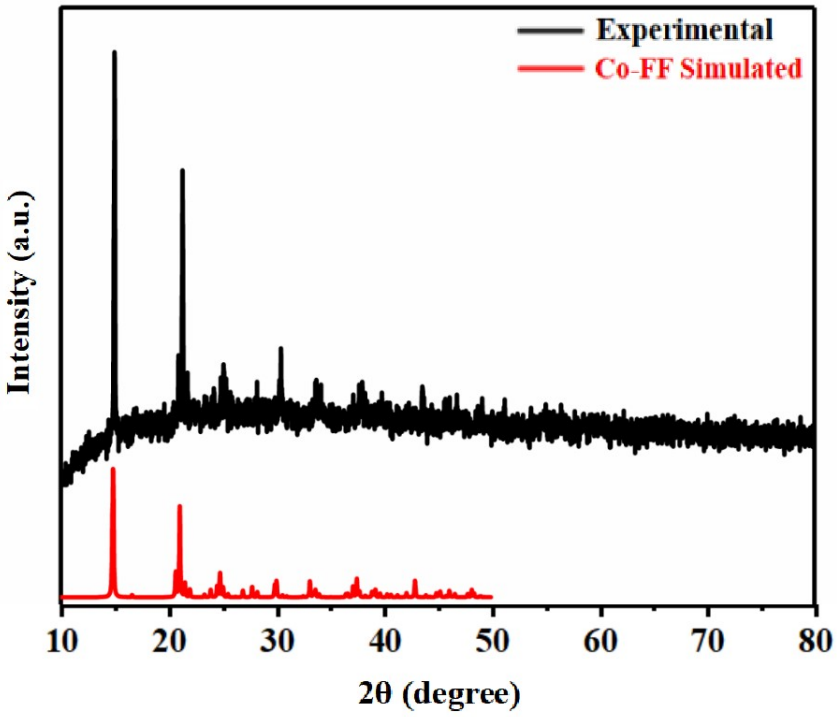

Figure S7. XRD pattern of Co-FF.

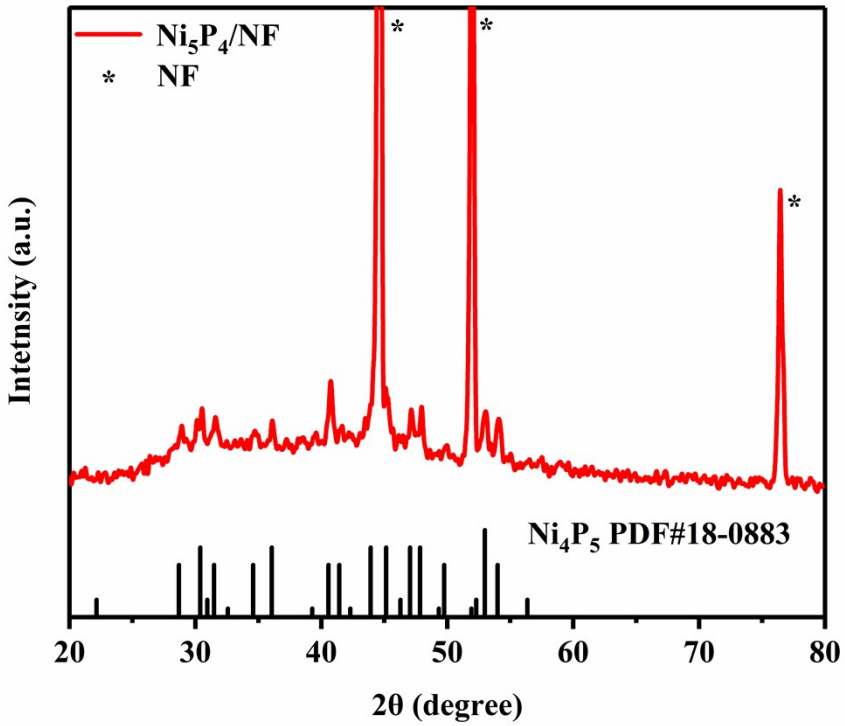

Figure S8. XRD pattern of Ni_5P_4/NF.

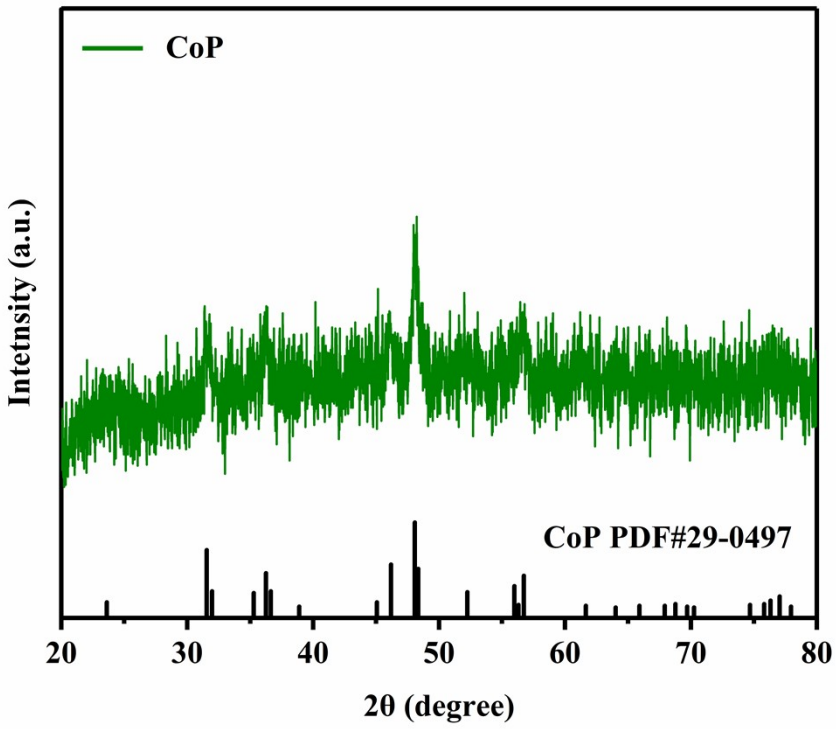

Figure S9. XRD pattern of CoP.

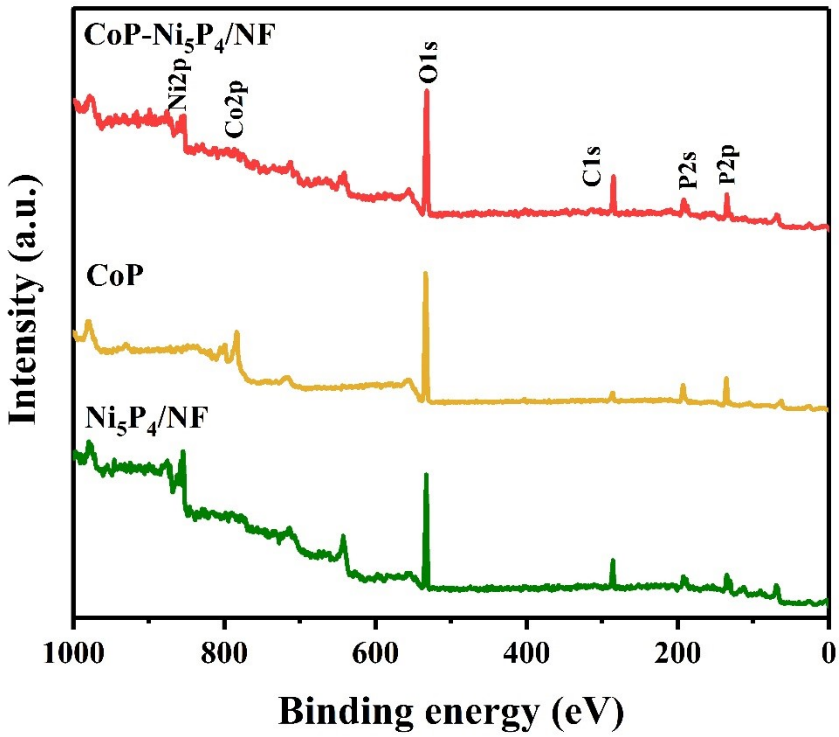

Figure S10. XPS survey spectra of CoP-Ni_5P_4/NF, CoP and Ni_5P_4/NF.

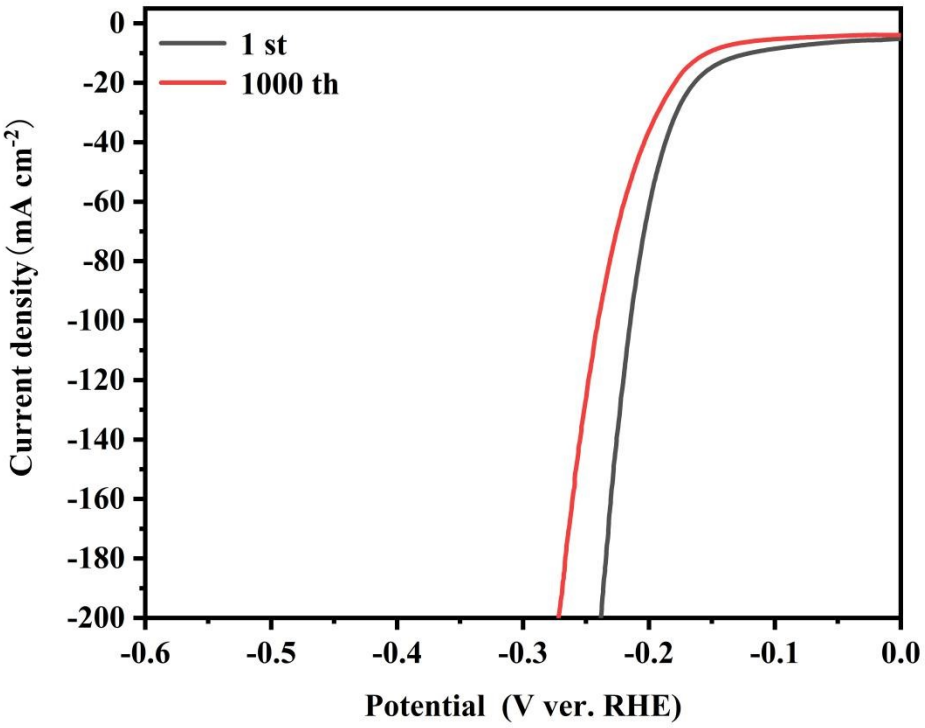

Figure S11. The LSV curves of CoP-Ni_5P_4/NF before and after 1000 CV cycles for HER.

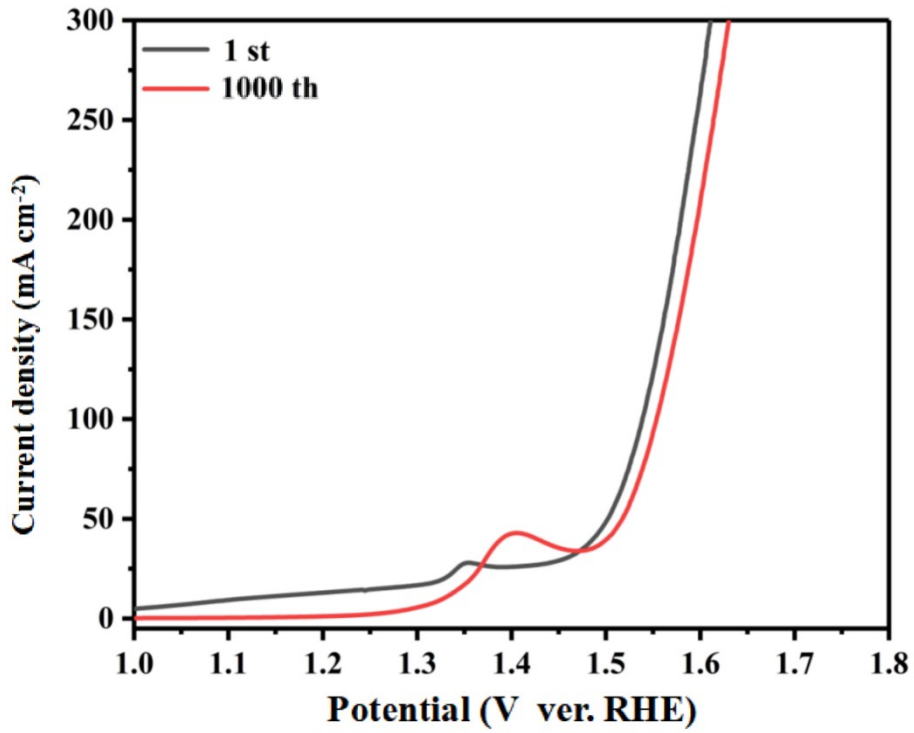

Figure S12. The LSV curves of CoP-Ni_5P_4/NF before and after 1000 CV cycles for OER.

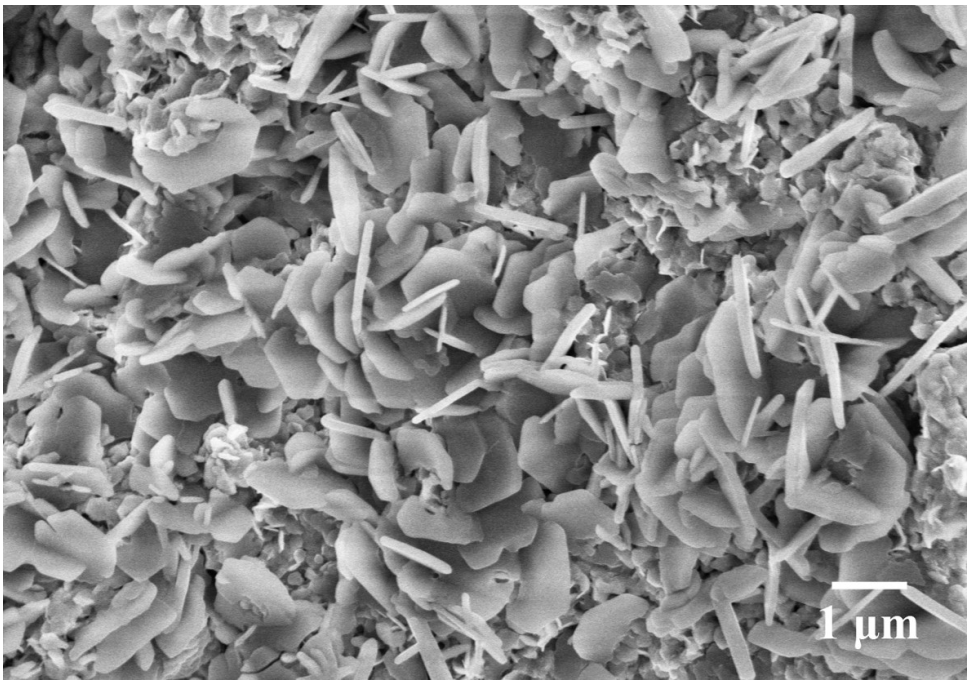

Figure S13. SEM image of CoP-Ni_5P_4/NF after the *I-t* test for HER.

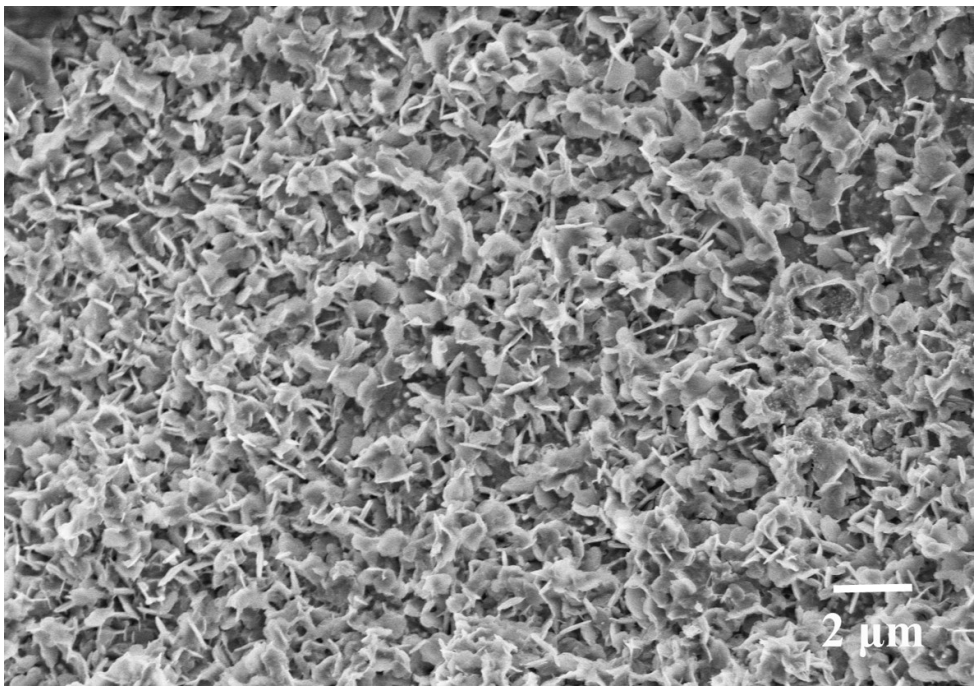

Figure S14. SEM image of CoP-Ni_5P_4/NF after the *I-t* test for OER.

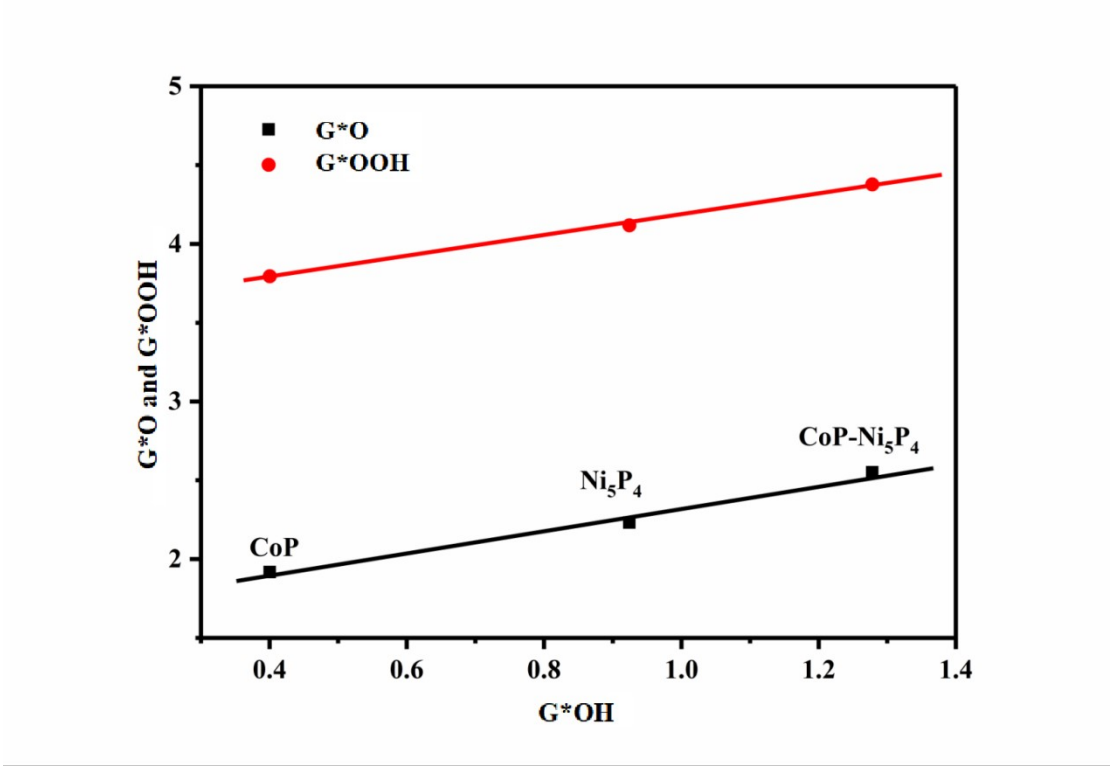

Figure S15. The linear scaling relation of the adsorption free energy between *OH and *O, *OOH intermediates in the OER reaction for CoP, Ni_5P_4 and CoP-Ni_5P_4.

Table S1. Comparison of HER activities of CoP-Ni_5P_4/NF with other reported TMPs electrocatalysts

Catalysts	***J*** **(mA cm^{-2})**	**Overpotential (mV)**	**Tafel slope (mV dec^{-1})**	**Reference**
CoP-Ni_5P_4/NF	10	125	109	This work
NiCoP-C(TPA)/NF	10	78	73.4	[7]
CoP/BMHNC	10	95.8	33	[8]
Multishelled Ni_2P	10	98	86.4	[9]
CoP@NF	10	100	57	[10]
Ti_3C_2@mNiCoP	10	127	103	[11]
FeNiP/NPCS	10	181	111	[12]
$(Fe_{0.1}Ni_{0.9})_2P(O)$/NF	10	87	47	[13]
(Fe-Co-Ni)P@PC/NF	10	134	75.7	[14]
FeP_2-NiP_2@PC	10	179	65	[15]

Table S2. Comparison of OER activities of CoP-Ni_5P_4/NF with other reported TMPs electrocatalysts

Catalysts	***J*** **(mA cm^{-2})**	**Overpotential (mV)**	**Tafel slope (mV dec^{-1})**	**Reference**
CoP-Ni_5P_4/NF	50	223	71	This work
CoNiP@CN	30	258	81	[16]
N-NiCoP/NCF	10	225	46	[17]
$NiFeP_x$-80/NF	10	224	29	[18]
Ni-CoP@C	10	279	54	[19]
NiCoPO/NC	10	300	94	[20]
Ti_3C_2@mNiCoP	10	237	104	[11]
FeP_2-NiP_2@PC	10	248	54	[15]
MnCoP/CC	10	261	92.6	[21]

Table S3. Comparison of overall water splitting activities of CoP-Ni_5P_4/NF with other reported TMPs electrocatalysts

Catalysts (Cathode)	**Catalysts (anode)**	***J*** **(mA cm^{-2})**	**Potential (mV)**	**Reference**
CoP-Ni_5P_4/NF	CoP-Ni_5P_4/NF	10	1.47	This work
FeP/Ni_2P	FeP/Ni_2P	10	1.42	[22]
Ni_2P/CP	Ni_2P/CP	10	1.57	[9]
Fe-CoP/Ti	Fe-CoP/Ti	10	1.6	[23]
CoNiP@CN/NF	CoNiP@CN/NF	30	1.59	[16]
N-NiCoP/NCF	N-NiCoP/NCF	10	1.56	[17]
CoP-N/Co foam	CoP-N/Co foam	50	1.61	[24]
Ni_5P_4|Fe	Ni_5P_4|Fe	10	1.59	[25]
$(Fe_{0.1}Ni_{0.9})_2P(O)$/NF	$(Fe_{0.1}Ni_{0.9})_2P(O)$/NF	10	1.50	[13]
NiCoP	NiCoP	10	1.51	[26]

Reference:

[1] M. D. Segall, P. J. D. L. M. J. Probert, C. J. Pickard, P. J. Hasnip, S. J. Clark and M. C. Payne, J. Phys. Condens. **2002**, 14, 2717.

[2] J. P. Perdew, K. Burke and M. Ernzerhof, Phys. Rev. Lett. **1996**, 77, 3865.

[3] D. R. Hamann, M. Schl¨ uter and C. Chiang, Phys. Rev. Lett. **1979**, 43, 1494.

[4] H Nakai, J Heyd, GE Scuseria, J. Comput. Chem. **2006**, 27, 1787–1799.

[5] Y. Li, Q. Zhang, C. Li, H. N. Fan, W. B. Luo, H. K. Liu, S. X. Dou, J. Mater. Chem. A **2019**, 7, 22242;

[6] Y. Wu, C. Li, W. Liu, H.H. Li, Y. Y. Gong, L. Y. Niu, X. J. Liu, C. Q, Sun and S. Q. Xu, Nanoscale **2019**, 11, 5064.

[7] S. Sirisomboonchai, S. S. Li, A. Yoshida, S Kongparakul, C. Samart, Y. Kansha, X. G. Hao, A. Abudula, G.Q. Guan, Catal. Sci. Technol. **2019**, 9, 4651.

[8] W. Y. Yuan, X. Y. Wang, X. L. Zhong, C. M. Li, ACS Appl. Mater. Interfaces **2016**, 8, 20720.

[9] H. M. Sun, X. B. Xu, Z. H. Yan, X. Chen, F. Y. Cheng, P. S. Weiss, J. Chen, Chem. Mater. **2017**, 29, 8539.

[10] B. L. Qiu, A. Han, D. H. Jiang, T. T. Wang, P. W. Du, ACS Sustain. Chem. Eng. **2019**, 7, 2360.

[11] Q. Yue, J. Sun, S. Chen, Y. Zhou, H. J. Li, Y. Chen, R. Y. Zhang, G. F. Wei, Y. J. Kang, ACS Appl. Mater. Interfaces. **2020**, 12, 18570.

[12] J. T. Ren, Y. S. Wang, L. Chen, L. J. Gao, W. W. Tian, Z. Y. Yuan, Chem. Eng. J. **2020**, 389, 124408.

[13] C. Lin, D. Q. Wang, H. H. Jin, P. Y. Wang, D. Chen, B. S. Liu, S. C. Mu, J.

Mater. Chem. A **2020**, 8, 4570.

[14] Y. X. Zhu, L. Zhang, G. G. Zhu ,X. Zhang, S. Y. Lu, J. Colloid Interface Sci. **2020**, 562, 42.

[15] P. X. Ji, H. H. Jin, H. L. Xia, X. Luo, J. K. Zhu, Z. H. Pu ,S. C. Mu, ACS Appl. Mater. Interfaces **2020**, 12, 727.

[16] L. Y. Yang, L. Zhang, Appl. Catal. B-Environ. **2019**, 259, 118053.

[17] R. Zhang, J. Huang, G. L. Chen, W. Chen, C. S. Song, C. R. Li, K. Ostrikov, Appl. Catal. B-Environ. **2019**, 5, 414.

[18] B. B. Yuan, F. Z. Sun, C. Q. Li, W. Huang, Y. Q. Lin, Electrochim. Acta **2019**, 313, 91.

[19] X. T. Han, C. Yu, H. W. Huang, W. Guo, C. T. Zhao, H. L. Huang, S. F. Li, Z. B. Liu, X. Y. Tan, Z. M. Gao, J. H. Yu, J. S. Qiu, Nano Energy **2019**, 62, 136.

[20] C. S. Wang, W. B. Chen, D. Yuan, S. S. Qian, D. D. Cai, J. T. Jiang, S. Q. Zhang, Nano Energy **2020**, 69, 104453.

[21] M. S. Wang, W. Y. Fu, L. Du, Y. S. Wei, P. Rao, L. Wei, X. S. Zhao, Y. Wang, S. H. Sun, Appl. Surf. Sci. **2020**, 15, 146059.

[22] F. Yu, H. Q. Zhou, Y. F. Huang, J. Y. Sun, F. Qin, J. M. Bao, W. A. Goddard, S. Chen, Z. F. Ren, Nat. Commun. **2018**, 9, 2551.

[23] C. Tang, R. Zhang, W. B. Lu, L. B. He, X. Jiang, A. M. Asiri, X. P. Sun, Adv. Mater. **2016**, 29, 102441.

[24] Z. Liu ,X. Yu, H. G. Xue, L. G. Feng, J. Mater. Chem. A **2019**, 7, 13242.

[25] J. L. Qi, T. X. Xu, J. Cao, S. Guo, Z. X. Zhong, J. C. Feng, Nanoscale **2020**,

12, 6204.

[26] X. D. Lv, X. T. Li, C. Yang, X. Q. Ding, Y. F. Zhang, Y. Z. Zheng, S. Q. Li, X. N. Sun, X. Tao, Adv. Funct. Mater. **2020**, 30, 1910830.